

LABORATOIRE EUROPEEN POUR LA PHYSIQUE DES PARTICULES (CERN)

EPS 0416

PA-09

PL-12

Search for scalar top quarks in e^+e^- collisions
at LEP1 energies

The ALEPH Collaboration

OPEN-99-128
06/09/99**Abstract**

The supersymmetric partners of the quarks, called squarks, are commonly believed to be out of the reach of LEP1. However, because of the large top quark mass, the mixing between the “left-handed” and “right-handed” stops can be substantial, and the lighter mass eigenstate could be light enough to be pair-produced at LEP1 energies. Moreover, the coupling of the stop to the Z can be suppressed for certain values of the mixing angle. The negative chargino searches imply that the decay $\tilde{t} \rightarrow \chi^+ b$ is forbidden. The stop then decays into χc via a loop, with a lifetime long enough for the stop to hadronize into a stop-hadron before decaying, in contrast to other squarks. Stop pair production in e^+e^- collisions, where the stop decays into χc , has been searched for in 140 pb^{-1} of data at and around the Z peak collected by the ALEPH detector until 1994. No signal was observed and exclusion domains result, presented as a function of the stop mass, the χ mass and the mixing angle in the stop sector.

*Contribution to the International Europhysics Conference on High Energy Physics
Brussels, Belgium, July 27-August 2, 1995*

1 Introduction

Scalar quarks are excluded by experiments at hadron colliders well beyond the mass domain accessible at LEP [1]. Typically, however, these exclusions apply under hypotheses such as mass degeneracy of five flavour species and of left and right partners of ordinary quarks, which in effect means ten degenerate scalar quark species. The mass splittings between the various scalar partners of the five lightest quarks may indeed be expected to be negligible for those analyses in the context of minimal supergravity models. However, it is also expected that the scalar partners of the top quark might be substantially lighter, due to the effect of the large top quark Yukawa coupling in the renormalization group equations. Moreover, while the mass eigenstates are expected to be almost identical to the electroweak interaction eigenstates in the case of scalar partners of light quarks, this is no longer true for the two scalar partners of the top. This feature is due to potentially large off-diagonal entries in the scalar top mass matrix related to the large value of the top quark mass:

$$M = \begin{pmatrix} m_{\tilde{t}_L}^2 & m_t a \\ m_t a & m_{\tilde{t}_R}^2 \end{pmatrix}$$

where the a parameter is typically expected to be of the same order as the scalar quark masses. It could therefore very well be that one of the scalar partners of the top quark, hereafter called “stop”, is much lighter than all the other scalar quarks. The stop is a mixture of the weak eigenstates

$$\tilde{t} = \tilde{t}_L \cos \theta_t + \tilde{t}_R \sin \theta_t \quad ,$$

defined by the mixing angle, θ_t .

The fact that the stop is not a weak eigenstate has important consequences for its production cross-section at LEP1 energies. The $Z\tilde{t}\tilde{t}$ coupling is proportional to

$$\frac{1}{2} \cos^2 \theta_t - \frac{2}{3} \sin^2 \theta_W \quad ,$$

which implies that the stop decouples from the Z for $\theta_t \sim 0.98$ rad. Even in that case, however, stops can be pair produced by photon exchange, but with a much reduced rate. The cross-section used in this analysis is taken from Ref. [2], where the leading order QCD corrections are given. In addition, QED corrections calculated to second order with soft photon exponentiation are applied.

In the stop mass domain accessible at LEP1 energies, the direct decays $\tilde{t} \rightarrow t\chi$ and $\tilde{t} \rightarrow b\chi^+$ are kinematically forbidden. The dominant decay mode is thus $\tilde{t} \rightarrow c\chi$ which proceeds *via* loop diagrams. The stop lifetime [2] then turns out to be larger than the hadronization time, and this is taken into account in the present analysis in the following way. Stops first hadronize as if they were ordinary quarks, using the JETSET model with a Peterson *et al.* fragmentation function controlled by a parameter scaled from b-quarks

$$\epsilon_{\tilde{t}} = \epsilon_b \frac{m_b^2}{m_{\tilde{t}}^2} \approx 0.006 \frac{m_b^2}{m_{\tilde{t}}^2} .$$

Stop hadrons then decay according to $\tilde{t} \rightarrow c\chi$, following a simple spectator model. The lightest neutralino, χ , is assumed to be the lightest supersymmetric particle, stable by R-parity conservation.

The results reported here were obtained using a sample of 140 pb^{-1} accumulated by the ALEPH detector at LEP, at energies at and close to the Z peak, during the years 1989 to 1994. This data sample contains approximately 3.7 million hadronic Z decays. Descriptions of the ALEPH detector, of the relevant trigger conditions and of the algorithms used in the analysis can be found in Refs. [3], [4] and [5], respectively. In order to design the selection criteria, many signal Monte Carlo samples, corresponding to various doublets of stop and χ masses, were used. These were obtained with a fast simulation program, calibrated to reproduce the results of full simulations performed for fewer mass doublets. Full simulations were in particular performed close to the boundaries of the sensitivity domain. In addition, large fully simulated Monte Carlo samples were used for all standard background processes (two and four-fermion final states).

2 Event selections

Events resulting from the production of a stop pair are expected to show as a pair of acoplanar (c-quark) jets, with missing energy taken away by the two χ s. Such an acoplanar jet topology has already been investigated [6] in the context of the search for the standard model Higgs boson produced in association with a $\nu\bar{\nu}$ pair (“ $H\nu\bar{\nu}$ ” analysis). The efficiency of that search applied to stops is 24% for $m_{\tilde{t}} = 42 \text{ GeV}/c^2$ and $m_{\chi} = 2 \text{ GeV}/c^2$. The $H\nu\bar{\nu}$ analysis was optimized for the case of a heavy Higgs boson, leading to not violently acollinear hadronic jets with a large visible mass. Here, the situation is easier in a large fraction of the $(m_{\tilde{t}}, m_{\chi})$ parameter space where typically more than half of the centre of mass energy escapes undetected. This allows simpler and, in some configurations, more efficient selection criteria to be designed.

Only events with at least four charged particle tracks are considered. Most of the $q\bar{q}$ background is rejected by the requirement that the visible mass should be smaller than $50\%\sqrt{s}$. Events with an angle θ_T of the thrust axis with respect to the beam axis such that $|\cos\theta_T| > 0.9$ are eliminated, and so are events with energy detected within 12° from the beam axis as in both cases additional energy is likely to have escaped down the beam pipe. The bulk of the $\gamma\gamma$ background is rejected by the requirement that the component of the total visible momentum transverse to the beam axis should exceed $5\%\sqrt{s}$.

Each event is divided into two hemispheres by a plane perpendicular to the thrust axis. The acollinearity angle is defined as the angle between the two hemisphere momenta, and the acoplanarity angle as that between those momenta projected onto the plane perpendicular to the beam axis. The remaining events are then classified as *i*) high multiplicity events, with more than seven charged particle tracks, in which the main background is still $q\bar{q}$ events (mostly with heavy quark semileptonic decays), and *ii*) low multiplicity events where $\gamma\gamma$ events and tau pairs dominate.

Masses		Efficiencies in per cent			
$m_{\tilde{t}}$	m_{χ}	H $\nu\bar{\nu}$	High mult.	Low mult.	total
45	42	0	0.1	0.6	0.7
45	40	0	4.3	12.0	16.3
45	25	14.0	30.6	9.4	54.0
45	02	22.2	33.4	5.3	60.9
42	32	3.0	20.7	13.6	37.3
30	28	0.2	0.2	0.6	1.0
30	26	0.2	5.2	9.9	15.3
30	15	24.1	11.8	6.6	42.5
20	10	21.6	5.9	5.5	33.0
10	06	3.3	0.3	0.4	4.0
5	2	0.7	0	0	0.7

Table 1: Analysis efficiencies. The efficiency of the High multiplicity analysis is to be added to that of the H $\nu\bar{\nu}$ one, and that of the Low multiplicity analysis to the sum of the two others.

In the high multiplicity sample, the acollinearity and the acoplanarity angles are required to be smaller than 135° and 150° , respectively. The effect of the acoplanarity cut is shown in Fig. 1. In addition, after forcing the jet algorithm to reconstruct exactly three jets, the sum of all three jet-jet angles is required to be greater than 350° . (The selectivity of this variable against the $q\bar{q}$ background has been demonstrated in the H $\nu\bar{\nu}$ analysis.)

In the low multiplicity sample, the thrust axis is required to form an angle of at least 45° with respect to the beam axis, which takes advantage of the $\sin^2\theta$ angular distribution of the signal. For “monojet” events, *i.e.* events in which one of the hemispheres is empty, it is further required that the visible mass be in excess of $5 \text{ GeV}/c^2$ and the value of the thrust lower than 0.95; these cuts eliminate the $\gamma\gamma$ and $\tau^+\tau^-$ backgrounds. For non-monojet events, it is required that each hemisphere contain at least two charged particle tracks and that the acoplanarity angle be lower than 150° (Fig. 1), thus eliminating the remaining $\tau^+\tau^-$ background.

No events were selected in the data, neither by the H $\nu\bar{\nu}$ analysis nor by any of the “High multiplicity” or “Low multiplicity” analyses described above. Based on studies of the standard background Monte Carlo samples, less than 1.7 events were expected to be selected. In Table 1, the cumulative efficiencies of these three analyses are given for various configurations of the stop and χ masses. As soon as the difference Δm between the stop and χ masses exceeds $5 \text{ GeV}/c^2$, the total efficiency is larger than 10% and increases with Δm and with the stop mass.

In order to increase the sensitivity in the region of small Δm , a complementary analysis has been designed, but this time not expected to be free of standard backgrounds (mostly from $\gamma\gamma$ interactions). Here too, the visible mass should be lower than $50\%\sqrt{s}$ and no

energy should be detected within 12° from the beam axis. The total visible energy is required to be greater than 3 GeV and the missing momentum should point more than 55° away from the beam axis. Each of the event hemispheres is required to contain at least two charged particle tracks and both hemisphere momenta should point more than 45° away from the beam axis. Finally, the acoplanarity angle should not exceed 135° (Fig. 1). Fourteen events were selected in the data, which is compatible with the expectation from $\gamma\gamma$ processes. The efficiency of these criteria is of a few per cent for Δm as low as $2 \text{ GeV}/c^2$.

3 Results

The accurate Z width measurement at LEP allows limits on stop pair production in Z decays to be set, which translate into stop mass upper limits as a function of the stop mixing angle as shown in Fig. 2. (A maximum of 23 MeV has been allowed, at the 95% confidence level, for a possible contribution from non standard processes to the Z width.) These limits are independent of the stop decay pattern, and in particular of the χ mass.

These exclusion domains can be extended by the analyses described in the previous section. In order to accommodate the various systematic errors (of which the largest come from the limited Monte Carlo statistics, from uncertainties in the stop fragmentation model and from the trigger simulation), the efficiencies have been reduced by 10%. A first exclusion domain is obtained by the combination of the three background free selections (H $\nu\bar{\nu}$, High and Low multiplicity). This domain is extended for low Δm values by the use of the complementary dedicated selection instead, considering the fourteen candidate events as possible signal events. The results are shown in the $(m_{\tilde{t}}, m_\chi)$ plane in Fig. 3, for a pure \tilde{t}_L ($\theta_t = 0$), for a pure \tilde{t}_R ($\theta_t = \pi/2$), and for a stop fully decoupled from the Z. They are also shown in Fig. 2 in the $(m_{\tilde{t}}, \theta_t)$ plane for $\Delta m \geq 2$ and $\Delta m \geq 5 \text{ GeV}/c^2$.

It can be seen that stops are excluded up to the kinematic limit, unless the stop- χ mass difference Δm is very small and, at the same time, the mixing angle θ_t is such that the stop decouples from the Z. These results improve somewhat on those reported earlier by the OPAL collaboration [7]. Recently, the D0 collaboration at the Tevatron has excluded a stop mass region extending approximately from 50 to 100 GeV/c^2 , *i.e.* not overlapping with the LEP1 search domain, and for Δm exceeding $\sim 30 \text{ GeV}/c^2$ [8].

References

- [1] See for instance: S.Hagopian *in* Proc. of the XXVIIth Int. Conf. on High Energy Physics, Glasgow, Scotland, 20-27 July 1994, eds. P.J. Bussey and I.G. Knowles, p.809.
- [2] M. Drees and K. Hikasa, Phys. Lett. **B 252** (1990) 127.
- [3] ALEPH Coll., D. Decamp *et al.*, Nucl. Inst. and Methods **A 294** (1990) 121.
- [4] ALEPH Coll., D. Decamp *et al.*, Phys. Rep. **216** (1992) 253.
- [5] ALEPH Coll., D. Buskulic *et al.*, Nucl. Inst. and Methods **A 360** (1995) 481.
- [6] ALEPH Coll., “Improved Mass Limit for the Standard Model Higgs Boson”, Contribution EPS0414 to the International Europhysics Conference on High Energy Physics, Brussels, Belgium, July 27-August 2, 1995.
- [7] OPAL Coll., R. Akers *et al.*, Phys. Lett. **B 337** (1994) 394.
- [8] D0 Coll., “Search for Light Top Squarks with the D0 detector”, presented at the 10th Topical Workshop on Proton Antiproton Collider Physics, Batavia, IL, 9-13 May 1995; and Contribution EPS0435 to the International Europhysics Conference on High Energy Physics, Brussels, Belgium, July 27-August 2, 1995.

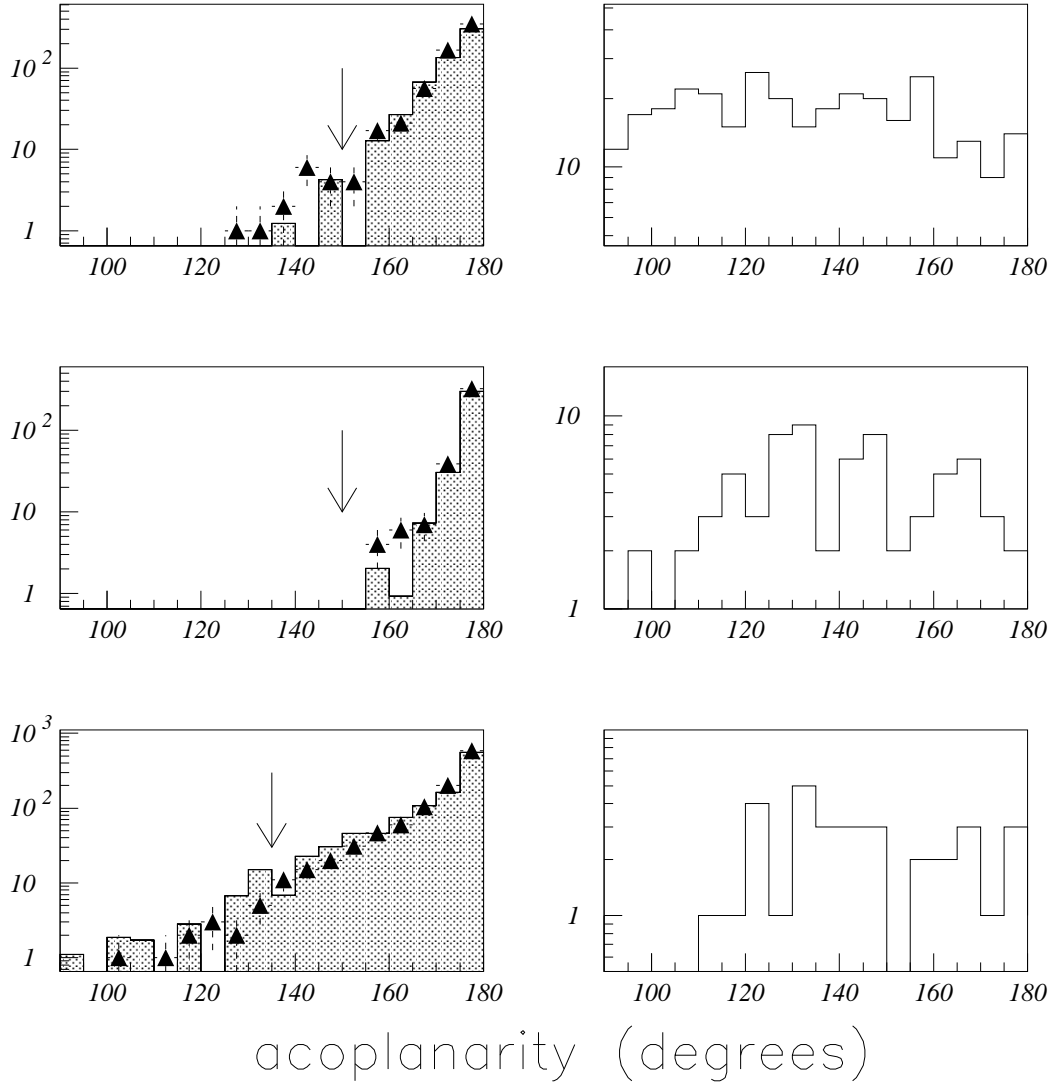


Figure 1: Distribution of the acoplanarity angle in the High multiplicity analysis (top), in the Low multiplicity analysis (middle) and in the complementary analysis (bottom). On the left side, the data are represented by points with error bars and the background expected from standard processes by shaded histograms; the cut locations are indicated by arrows. On the right side, the corresponding expected signal distributions are shown for $m_{\tilde{t}}=45$ and $m_{\chi}=25$ GeV/c^2 (top), for $m_{\tilde{t}}=30$ and $m_{\chi}=27$ GeV/c^2 (middle), and for $m_{\tilde{t}}=42$ and $m_{\chi}=40$ GeV/c^2 (bottom).

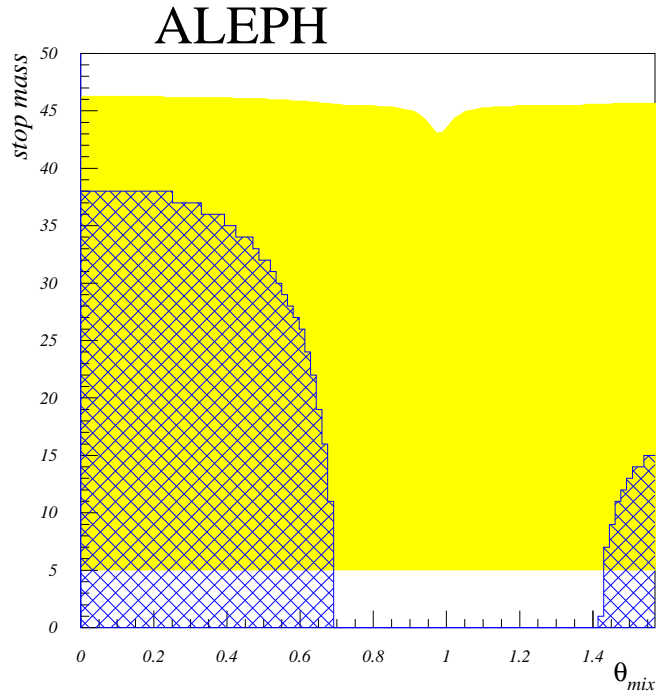
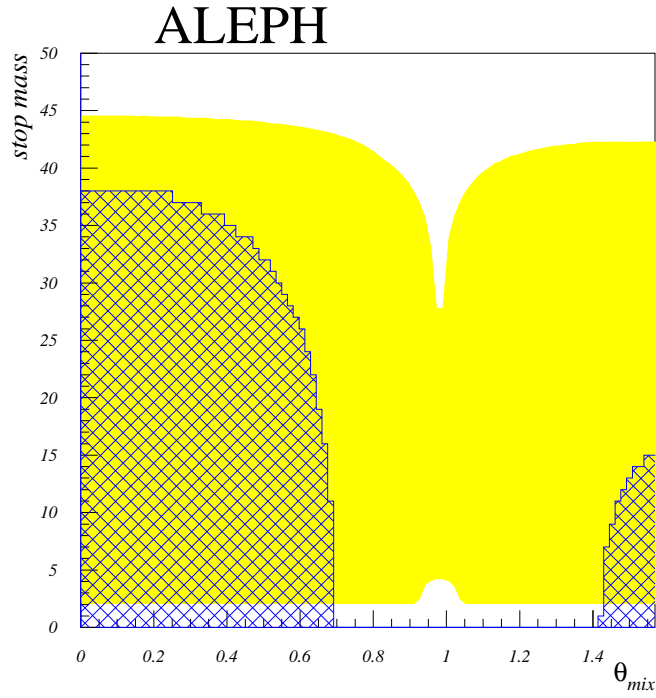


Figure 2: 95% C.L. excluded domains in the $(m_{\tilde{t}}, \theta_t)$ plane for two values of Δm . The hatched areas are excluded by the Z width constraint.

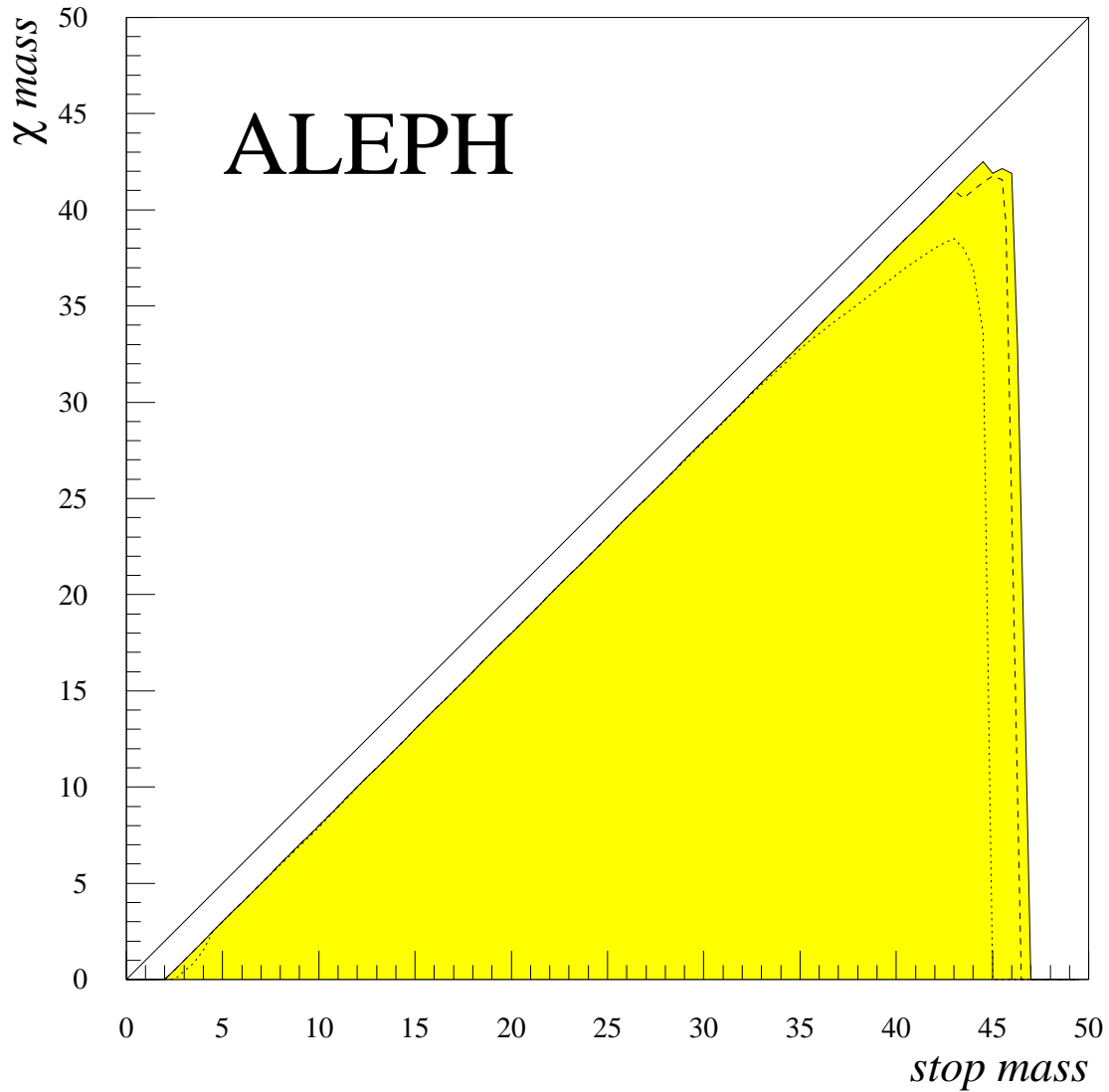


Figure 3: 95% C.L. excluded domains in the $(m_{\tilde{t}}, m_{\chi})$ plane, for three values of θ_t . The outermost (continuous) contour corresponds to $\theta_t = 0$, the intermediate (dashed) one to $\theta_t = \pi/2$, and the innermost (dotted) one to a stop fully decoupled from the Z ($\cos^2 \theta_t = (4/3) \sin^2 \theta_W$).